nature physics

SUPPLEMENTARY INFORMATION

DOI: 10.1038/NPHYS1366

Supplementary Information for "Locking electron spins into magnetic resonance by electron-nuclear feedback"

Ivo T. Vink, Katja C. Nowack, Frank H. L. Koppens, Jeroen Danon, Yuli V. Nazarov, and Lieven M. K. Vandersypen
Kavli Institute of Nanoscience, Delft University of Technology, PO Box 5046, 2600 GA Delft, The Netherlands

(Dated: June 1, 2009)

TUNING THE DOUBLE DOT

The conditions for observing a pronounced electron-nuclear feedback are as follows. Qualitatively, the interdot tunnel coupling and the tunnel coupling to the outgoing lead are increased compared to the regime of Ref. [1]. Furthermore, the potentials of the double dot are tuned such that the interdot transition occurs without energy loss: at low power, the configuration of the dot potentials is such that electrons can tunnel elastically from the left to the right dot when spin blockade is lifted. Thereby, the interdot transition is made from the $(1,1)$ singlet to the $(0,2)$ singlet, where (m,n) represent the effective electron numbers on the two dots. This working point cannot be used at strong driving, since the electric field component of the excitation causes photon assisted tunneling to the $(0,2)$ triplet, thereby lifting spin blockade irrespective of the spin states of the two electrons. Instead, the double dot must be tuned such that the $(0,2)$ singlet electrochemical potential is higher than that of the $(1,1)$ singlet. This is nominally in the Coulomb blockade regime, but photon-assisted tunneling now provides the missing energy in order to make the transition from the $(1,1)$ to the $(0,2)$ singlet.

SUPPRESSION OF FLUCTUATIONS

In this section we derive an estimate for the typical magnitude of nuclear field fluctuations around a stable point close to resonance. For the sake of argument we show here the derivation for a *single* quantum dot, although a similar argument holds for a double dot setup and the results are qualitatively similar as well. (in the double dot case, a *two dimensional* Fokker-Planck equation must be considered, where stable points correspond to zeros of $\{\partial_t x_1, \partial_t x_2\}$ in the plane (x_1, x_2))

We consider all possible configurations of the nuclear spin system in the dot as discrete points, labeled n, defining $n \equiv \frac{1}{2}(N_+ - N_-)$, where $N_{+(-)}$ denotes the number of nuclei with spin up(down) [2]. This results in $N \equiv N_+ + N_-$ possible values for n, ranging from $-N/2$ to $N/2$. To investigate the stochastic properties we derive a Fokker-Planck equation for the probability distribution function $\mathcal{P}(n)$, starting from a simple master equation

$$\frac{\partial \mathcal{P}(n)}{\partial t} = -\mathcal{P}(n)[\Gamma_+(n) + \Gamma_-(n)] + \mathcal{P}(n-1)\Gamma_+(n-1) + \mathcal{P}(n+1)\Gamma_-(n+1). \tag{1}$$

In this equation $\mathcal{P}(n)$ gives the chance of finding the system in state n, and $\Gamma_\pm(n)$ is the rate at which the spin bath flips from the configuration n to $n \pm 1$. We go over to the continuous limit, justified by the large number of nuclei $N \sim 10^6$ [3], and expand all functions around n up to second order. We find

$$\frac{\partial \mathcal{P}}{\partial t} = \frac{\partial}{\partial n}\left\{(\Gamma_- - \Gamma_+)\mathcal{P} + \frac{1}{2}\frac{\partial}{\partial n}(\Gamma_- + \Gamma_+)\mathcal{P}\right\}, \tag{2}$$

a Fokker-Planck equation where all rates $\Gamma_\pm$ are still functions of n. Due to the large number of nuclei, the spin flip rates $\Gamma_\pm$ do not change on their full scale when increasing n by only ± 1 (the features of $\Gamma_\pm$ occur on the scale of the width of the resonance ~ 1 mT, whereas changing n by ± 1 corresponds to $IA/N \sim 5$ μT). This implies that $|\partial_n \Gamma_\pm| \ll \Gamma_\pm$, which allows us to neglect one of the cross terms resulting from the last term in (2).

In the resulting continuity equation, the right-hand side corresponds to the derivative of a probability flux. In equilibrium this probability flux must vanish, which enables us to write down a general equilibrium solution of (2). In terms of the bath polarization $x \equiv 2n/N$ this solution reads

$$\mathcal{P}(x) = \exp\left\{\int^x N \frac{\Gamma_+ - \Gamma_-}{\Gamma_+ + \Gamma_-} dx'\right\}. \tag{3}$$

DOI: 10.1038/NPHYS1366

Maxima and minima of this distribution are found at the zeros of the derivative of the exponent. Suppose the point x_0 is one of these solutions corresponding to a maximum of $\mathcal{P}(x)$ (i.e. the second derivative in the point x_0 is negative). We then expand the exponent of $\mathcal{P}(x)$ up to second order around the maximum, giving a Gaussian approximation for $\mathcal{P}(x)$,

$$\mathcal{P}(x) \approx \exp\left\{ \int^{x_0} N\frac{\Gamma_+ - \Gamma_-}{\Gamma_+ + \Gamma_-}dx' + \frac{N}{2}\frac{\partial}{\partial x}\frac{\Gamma_+ - \Gamma_-}{\Gamma_+ + \Gamma_-}\bigg|_{x_0}(x-x_0)^2 \right\} \equiv \mathcal{P}(x_0)\exp\left\{ -\frac{(x-x_0)^2}{2\sigma^2} \right\}, \tag{4}$$

where σ gives the width of the distribution. So we find that

$$\sigma^2 = \frac{1}{N}\left(-\frac{\partial}{\partial x}\frac{\Gamma_+ - \Gamma_-}{\Gamma_+ + \Gamma_-}\bigg|_{x_0} \right)^{-1} = \frac{1}{N}\frac{\Gamma_+ + \Gamma_-}{\frac{\partial}{\partial x}(\Gamma_- - \Gamma_+)}\bigg|_{x_0}, \tag{5}$$

where we used that $(\Gamma_+ - \Gamma_-)|_{x_0} = 0$. We now only still want to translate this expression in terms of the 'pumping curve'. We use the relation $dx/dt = (2/N)(\Gamma_+ - \Gamma_-)$ and define $\gamma(x) = (2/N)(\Gamma_+ + \Gamma_-)$. In the limit of small polarizations, i.e. $|x| \ll 1$, we can write

$$\frac{dx}{dt} = L(x) - \gamma(x)x. \tag{6}$$

In this notation the effect of Γ_p (main text) is separated into two parts: (i) a polarization-dependent net spin pumping contribution, $L(x)$, and (ii) a polarization-dependent contribution to the relaxation, which together with the intrinsic relaxation rate $1/\tau_n$ is written as $\gamma(x)$. One can rewrite equation (5) in terms of dx/dt and $\gamma(x)$ using the relations given above. This gives us finally the expression

$$\sigma^2 \approx \frac{1}{N}\frac{\gamma(x_0)}{\left(-\frac{\partial}{\partial x}\frac{dx}{dt}\right)\big|_{x_0}}. \tag{7}$$

To get an idea of the magnitude of this variance, we approximate the derivative of the pumping curve at the stable point as roughly the height of $L(x)$ over the width (see Fig. 5 in the main text), i.e. $-\partial_x(dx/dt)|_{x_0} \approx L^{\max}/\tilde{x}$, where $\tilde{x}$ is the width of $L(x)$. From equation (6) we see that we can write for the absolute maximum of achievable polarization $x^{\max} = L^{\max}/\gamma(x^{\max})$. Combining these two expressions and using that $\gamma(x^{\max}) \sim \gamma(x_0)$, we find the order of magnitude of the variance σ^2 to be

$$\sigma^2 \sim \frac{1}{N}\frac{\tilde{x}}{x^{\max}}. \tag{8}$$

In terms of the effective nuclear field B_N, this variance reads

$$\sigma^2_{B_N} \sim \Omega^2\frac{B_1}{|B_N^{\max}|}, \tag{9}$$

where $\Omega \equiv IA/g\mu_B\sqrt{N}$ are the diffusive fluctuations around the unpolarized state, and B_1 is the scale of the width of the pumping term L, in our case given by the strength of the microwave driving field.

STATISTICS OF SWITCHING

Here we explain how we calculated the purple curve in Fig. 4e in the main text. We suggest that the second current jump (red diamonds in the Figure) corresponds to the resonance being lost in one of the two dots. This occurs when the effective barrier between the polarized and unpolarized states becomes small enough for a typical nuclear field fluctuation to overcome. If we assume a simple linear decrease of this effective barrier for increasing B_N and include the effect of the finite sweep rate $\dot{B}_0$, we find the polarization-dependent switching rate

$$\Gamma_{\rm sw}(B_N) = \Gamma_0\exp\left\{ \gamma\left(\frac{B_N}{B_N^{\max}} + \frac{\dot{B}_0}{\dot{B}_0^{\max}} \right) \right\}, \tag{10}$$

where $\dot{B}_0^{\max}$ is the maximal sweep rate to observe any locking at all. From this expression we can derive the standard deviation in B_N where the second jump is observed, $\sigma_{\rm sw}$, and the average switching field $\langle B_N^{\rm sw}\rangle$. Explicitly, we find

$$\sigma_{\rm sw} = \frac{B_N^{\max}}{\gamma} \qquad \text{and} \qquad \langle B_N^{\rm sw}\rangle = \sigma_{\rm sw} \ln \frac{\dot{B}_0^{\max}}{\sigma_{\rm sw}\Gamma_0} + \sigma_{\rm sw} \ln \frac{\dot{B}_0}{\dot{B}_0^{\max}} - B_N^{\max}\frac{\dot{B}_0}{\dot{B}_0^{\max}}. \tag{11}$$

We analyzed the set of red diamonds in Fig. 4e in the main text. From (11) we expect $\sigma_{\rm sw}$ to be constant in first approximation, which is indeed observed for lower sweep rates (100-400 mT/min). The decrease of $\sigma_{\rm sw}$ for sweep rates above 400 mT/min could be a consequence of the average switching field lying too close to the resonance condition. Therefore we averaged the standard deviation over the first four values to find $\sigma_{\rm sw} = 39$ mT. Using this value for the standard deviation, we fitted equation (11) to the data in Fig. 4e. This resulted in the fitting parameters $B_N^{\max} = 289.6$ mT, $\dot{B}_0^{\max} = 920.7$ mT/min and $\gamma = 6.946 \cdot 10^{-4}$ s^{-1}, giving a sample correlation coefficient of $R = 0.948$. The resulting fitting curve is plotted in purple in Fig. 4e. Another way to estimate $B_N^{\max}$ and $\dot{B}_0^{\max}$ is to extrapolate the set of red diamonds in Fig. 4e to the two axes. In this way one finds the estimates $B_N^{\max} \approx 300$ mT and $\dot{B}_0^{\max} \approx 900$ mT/min, both in reasonable agreement with the results of the fit.

ANALYSIS OF ESR CURRENT LEVELS

Next to the *position* of the current jumps, we also analyzed the *height* of the current plateaus between the jumps as function of driving amplitude. For different microwave powers we repeatedly swept the external magnetic field from low to high with a sweep speed of $\dot{B}_0 = 400$ mT/min, keeping the driving frequency fixed at $f = 400$ MHz. For each trace we averaged the current of the first plateau and the current of the second plateau, and we determined the height of the zero-field peak. The result is plotted in Figure 1 as a scatter plot for the different microwave powers. We clearly observe that in all traces the highest current was measured in the zero-field peak, and that the second plateau exhibited higher current than the first. As to the dependence of the current levels on driving power, we see that (i) the height of the zero-field peak tends to decrease with increasing excitation power and (ii) the height of the ESR current plateaus seems nearly constant. As we attribute the observed double step feature to dragging of the nuclear field, first in two and then only in one dot, we here give some general considerations concerning the current levels during resonant electron transport in double quantum dot ESR experiments.

Let us first consider the limit of strong microwave driving with a saturated ESR, i.e. $g\mu_B B_1/h$ much larger than all relaxation and decay rates. If *both* dots are exactly on resonance, the driving causes the electrons to evolve entirely within the triplet subspace [1], i.e. in the cycle $|T_+\rangle \to \frac{1}{2}\left\{|T_+\rangle + \sqrt{2}|T_0\rangle + |T_-\rangle\right\} \to |T_-\rangle \to \frac{1}{2}\left\{|T_+\rangle - \sqrt{2}|T_0\rangle + |T_-\rangle\right\} \to |T_+\rangle$. As all three $(1,1)$ triplet states are Pauli spin blockaded, current can only flow to the extent there is relaxation from the triplets to the singlet. If only *one* of the two dots is on resonance, the system will evolve due to driving in the cycle $|T_\pm\rangle \to \frac{1}{\sqrt{2}}\left\{|T_0\rangle \pm |S\rangle\right\} \to |T_\pm\rangle$, where in the course of every cycle the state $\frac{1}{\sqrt{2}}\left\{|T_0\rangle \pm |S\rangle\right\}$ can decay via the $(0,2)$ singlet to the outgoing lead, giving rise to a current. Therefore, we expect in this limit of strong driving to observe the highest current when only one dot is on resonance. Since the resonance is saturated in the strong driving regime, we expect to first approximation no dependence of the current on microwave power.

In the limit of very weak driving, with $g\mu_B B_1/h$ much smaller than the relevant rates, one would expect quite the opposite. In this case the system spends most time in a Pauli spin blockaded state. The blockade can be lifted by spin relaxation in one of the two dots or by a spin flip in either of the dots caused by the driving field B_1. In this limit we therefore expect increasing current with increasing driving power, and furthermore that current will be highest when both dots are on resonance, simply because more spin flips take place.

During a field or frequency sweep, it is in principle possible that a nuclear field builds up in only one dot when the nominal ESR condition is first reached, subsequently locking the dot to the ESR condition. However, it is very unlikely that a nuclear field would build up in the other dot at a later time, when the ESR frequency in that dot is very far away from the driving frequency. A much more likely scenario is that a nuclear field builds up in both dots when the ESR condition is first reached (first plateau, low current), and that at the second current jump, the polarization in one dot relaxes to zero and only the other dot polarizes further (second plateau, high current). This would suggest that our experiments were performed in the regime of strong driving.

However, there is an issue which does not fit in this simple picture. The decrease of the zero-field peak height for increasing power suggests that the electric field component of the excitation smears out the current peak in gate voltage space due to photon-assisted tunneling (at high frequencies, discrete sidebands are visible, at low frequencies, the sidebands overlap). This could account for the decrease of the zero-field current, but should presumably affect the ESR current levels in the same way since the ESR transition is saturated at strong driving. However, experimentally,

DOI: 10.1038/NPHYS1366

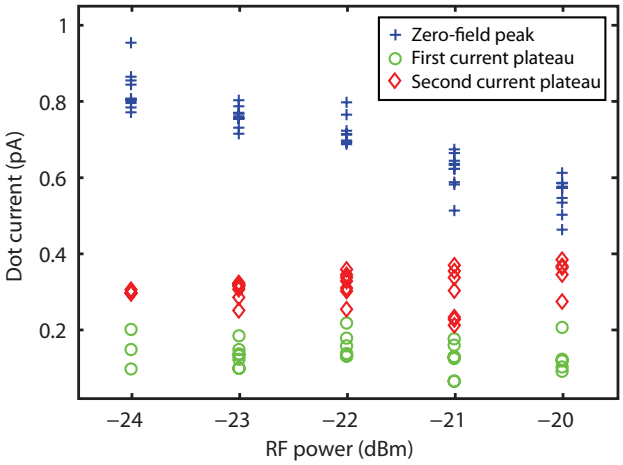

FIG. 1: Current levels of the zero-field peak and the two plateaus. An offset is subtracted from all current levels given by the average current between the tail of zero-field peak and the ESR resonance. The height of the zero-field peak is determined by averaging 3 points around the position of its maximum, which is determined by first averaging 10 consecutive measurements and determining the maximum current in the averaged trace. The current levels of the first plateau are obtained by averaging individual traces between the magnetic field values where the first step occurs (indicated by green circles in Fig. 4a in the main text) and the field where the second step occurs or the field value where the current drops to zero, if that occurs before the second step (red diamonds and black crosses in Fig. 4a in the main text). We require these magnetic field intervals to be longer than 10 measurement points (corresponding to 20mT) in order not to be omitted. The height of the second plateau is determined in a similar way but now by averaging between the magetic field values where the second step occurs and the field where the current drops to zero. The resulting heights of the zero-field peak, first and second current plateaus are represented here by respectively blue crosses, green circles and red diamonds for different excitation powers.

the current levels at the two ESR plateaus are roughly independent of power, rather than decreasing with power. This point remains at present unresolved.

In order to develop a coherent picture of electron transport at zero-field and at spin resonance, a more systematic and detailed study of the dependence of the current levels on driving power and on the tuning of the double dot (tunnel coupling, detuning) is needed. This is quite involved, since the behavior of even the zero-field peak varies widely with tuning parameters.

PUMP-PROBE MEASUREMENTS

Fig. 2 shows the full dataset for the pump-probe measurements presented in Fig. 3 of the main text, now including the pump phase ($t < 0$). The pump-phase data and accompanying discussion was left out from the main text for brevity. We note that the signal in the pump phase is much stronger than the signal in the probe phase, since during the pump phase a strong (-13dBm) continuous microwave excitation is applied, whereas during the probe phase, the excitation is applied only in bursts with a duty cycle of less than 10%. Even though the excitation is applied only in bursts, the electron spin sometimes remains locked into resonance during the probe phase as well, stalling the nuclear spin relaxation.

[1] F. H. L. Koppens, et al., Nature **442**, 766 (2006).
[2] We assume here for simplicity nuclear spin $I = 1/2$. For higher values of spin, e.g. $I = 3/2$ as in GaAs, the results do not change qualitatively.
[3] N. G. van Kampen, *Stochastic Processes in Physics and Chemistry* (North-Holland, Amsterdam, 1990).

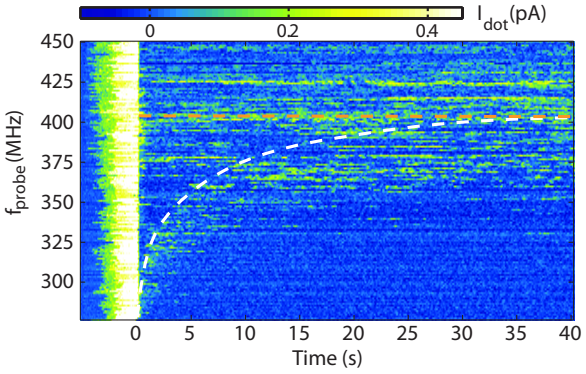

FIG. 2: Pump-probe measurement of the relaxation of the nuclear spin polarization. At a fixed magnetic field of $B_0 = 80$ mT, we apply CW excitation ($P = -13$ dBm) sweeping the frequency from 500 MHz to 276 MHz at 43 MHz/s, and dragging the nuclear field along (pump phase). Next we turn off the CW excitation and apply 140 ns microwave bursts every 2 μs at frequency $f_{\rm probe}$ throughout a 40 s probe phase. This pump-probe cycle is repeated for different probe frequencies, 277 MHz $\leq f_{\rm probe} \leq$ 450 MHz (see vertical axis). The horizontal axis indicates the time t into the probe phase; the data for $t < 0$ correspond to the pump phase. In the pump phase, the current (plotted in colorscale) jumps up twice, reaching the highest current plateau (traces where the resonance is lost by the end of the pump phase are left out). When the frequency is switched to $f_{\rm probe}$ at $t = 0$, the current drops to zero since the excitation is now off-resonance. As the nuclear spin polarization relaxes, the resonance condition $|g|\,\mu_B(B_0 + B_N(t)) = hf_{\rm probe}$ will be fulfilled at some point in time at which the current sets on again. Varying $f_{\rm probe}$ reveals then the nuclear spin relaxation as indicated by the white dashed line (guide to the eye) marking the onset of the current, where the probe pulses have had the least effect on the nuclear polarization. The orange dashed line marks an additional signal at the nominal resonance frequency already present from the start of the probe phase.